DALTON
FULL PAPER

Synthesis, structure and hydroformylation activity of monomer rhodium and iridium pyrimidine thiolate complexes

Sergio Rojas,[a] José Luis García Fierro,[a] Rosa Fandos,[b] Ana Rodríguez[c] and Pilar Terreros*[a]

[a] *Instituto de Catálisis y Petroleoquímica, CSIC, Campus UAM, Cantoblanco, 28049 Madrid, Spain. E-mail: pterreros@icp.csic.es*
[b] *Universidad de Castilla-La Mancha Departamento de Química Inorgánica, Orgánica y Bioquímica, Facultad de Ciencias del Medio Ambiente Toledo, Spain*
[c] *Departamento de Quimica Inorganica, Organica y Bioquimica, Escuela Técnica Superior de Ingenieros Industriales, Campus de Ciudad Real, 13071 Ciudad Real, Spain*

Received 28th February 2001, Accepted 25th May 2001
First published as an Advance Article on the web 17th July 2001

The reaction of dinuclear $[M(\mu\text{-Cl})(COD)]_2$ (M = Rh, Ir) with mercaptopyrimidine and its methylated derivatives affords monomeric complexes. Depending on the nature of the solvent used, the pyrimidine behaves as both a monodentate ligand, bonded to the metal directly through the sulfur atom, and as a bidentate ligand, bonded to the metal atom through both the sulfur and a nitrogen atom, acting as a chelating ligand. Reaction of these complexes with CO yields dicarbonyl complexes through displacement of the COD ligand. Displacement of one of the CO molecules occurs in the presence of PPh_3. Both rhodium and iridium phosphinated complexes may accept a second PPh_3 molecule within their coordination sphere, with no displacement of the remaining CO ligand. Thiolate rhodium complexes have proved to be good catalysts in the hydroformylation reaction of 1-heptene in the presence of PPh_3. The donor capacity of mercaptopyrimidine ligands has been correlated with the activity of the catalysts tested. In the present work, an increase in ligand basicity gave rise to a faster reaction. However, no significant modifications in the distribution of the final products were observed.

Introduction

Over the past few years considerable attention has been paid to the properties of metal thiolate complexes due to their numerous applications.[1] The chemistry of thiolates that incorporate heteroatoms, in particular N atoms, in their structure is of particular interest since such compounds display certain particular coordinating modes. In spite of the propensity of sulfur to stabilise metallic bridges,[2] S–N heterothiolates can coordinate as monodentate ligands[3] and, more frequently as polydentate ligands, both to one metal, acting as a chelating ligand,[3,4] or to several metal centres as a bridging ligand.[5] These polyfunctional ligands have been proposed as suitable candidates for the collection of early–late heterobimetallic complexes.[6] Pyrimidinethiol exhibits a tautomeric equilibrium in solution between the S (thiol) and N (thione) protonated forms.[7] Furthermore, at basic pH, non-protonated forms (thionate) predominate in the equilibrium.[7,8] [Fig. 1(a), (b) and (c), respectively].

Many complexes of monodentate, chelating and bridged heterothiolate ligands have been described.[3–5] If the heterothiolate ligand chelates the metal centre, four-, five- and six-coordinated complexes are known. Monosubstituted heterocyclic thionates are mainly S,N-chelating, thus generating four-membered ring species, although this kind of coordination is inherently strained because the S–M–N angle value is very low: typically around 70°.[9] When these ligands act in their protonated form, their coordination to the metal atom is generally through the sulfur atom.[10]

In recent years, the issue of hydroformylation, and carbonylation reactions in general, has been addressed in several reviews and books.[11] Thiolate–rhodium complexes are currently being studied extensively for use as catalysts in hydroformylation reactions.[12] Recently, it has been proposed that, under optimal conditions and with an appropriate bite angle and donor ability, the use of phosphines acting as chelating ligands appears to increase the *n*-octanal/internal aldehyde (n : i) mol ratio,[13] which is of great interest due to the highest value of the linear aldehyde. To our knowledge, phosphines are the only chelating donor ligands studied within this context. In the same vein, the basicity of the donor ligand appears to modify the reaction selectivity by varying the electron density at the metallic centre, although, again, it has only been studied with phosphine ligands. As a general trend, the greater the basicity of the phosphine derivative, the higher the n : i ratio.[14]

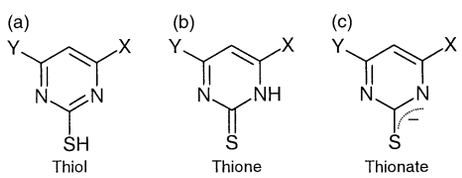

Fig. 1 Tautomeric forms of the thiopyrimidine ligands. The thionate name (c) is mantained, indicating thus its thione origin.

In the present work we focused on the synthesis, characterisation, reactivity and catalytic behaviour of rhodium and iridium pyrimidinethiolate complexes and their methylated derivatives. Different carbonylated, mono- and di-phosphinated rhodium thiolate complexes were tested in the hydroformylation of 1-heptene in order to correlate the basicity of the ligands with the behaviour of the catalysts, at the same time minimising the steric effects. Other reaction parameters such as the reaction pressure, the solvent and the effect of phosphine addition were also studied.

Results and discussion

Synthesis of pyrimidine thiolate complexes

Monomeric mercaptopyrimidine rhodium and iridium com-

 DOI: 10.1039/b101915p

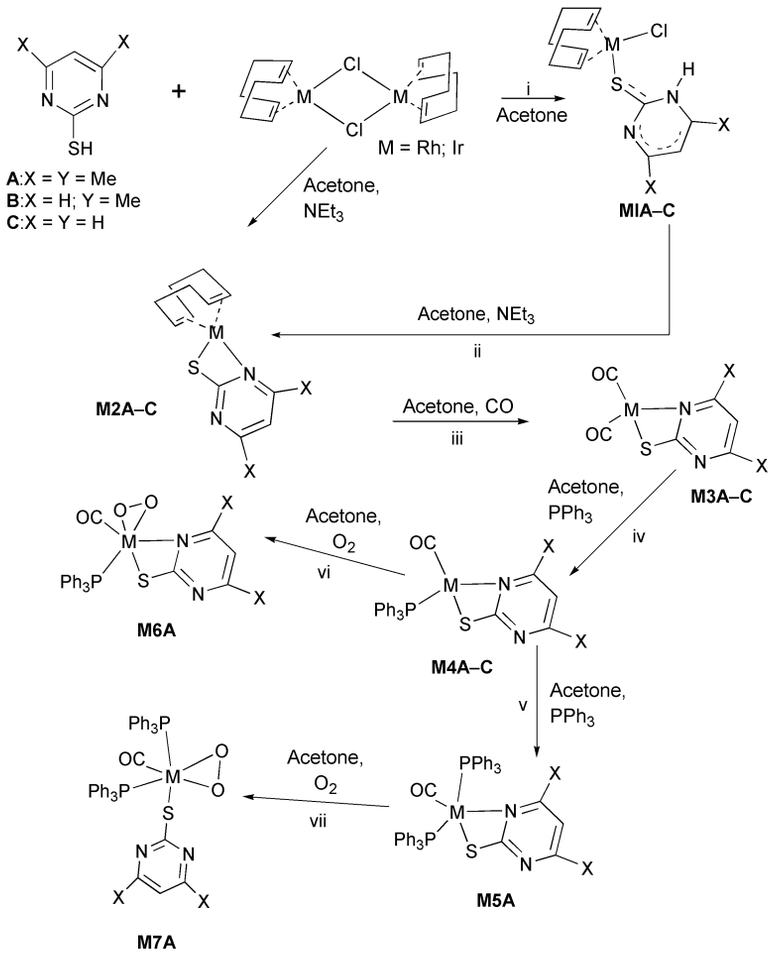

Scheme 1 Synthesis and reactivity of the pyrimidienethionate complexes of Rh and Ir.

plexes were prepared by reaction of the dimeric metallic precursors $[M(\mu\text{-Cl})(COD)]_2$ (M = Rh, Ir) with two equivalents of the corresponding pyrimidinethiols in organic or basic media. When the reaction took place in acetone, monomer complexes were obtained (Scheme 1, reaction i). The mercaptopyrimidine ligand behaved like a thione [Fig. 1(b)]. The sulfur atom is directly bonded to the metal centre. Monomeric tetracoordinated complexes were obtained, hereafter referred to as **M1A–C**, the ligands around the metal adopting a planar arrangement. In order to accomplish an accurate FTIR study of these complexes, the spectra were divided into four regions, I, II, III and IV, and the bands are listed in the Experimental section.[15] The evolution of the ligand bands was monitored and compared with that of the free ligand. For the **M1A–C** complexes, the displacement of the bands in region I to lower wavenumbers and the absence of displacement of the bands in region III were ascribed to S–M bond formation, without co-participation by the N atom.[16] In the ^{1}H NMR spectra of the most soluble complexes, generally the methylated ones, the methyl signals were not assigned unequivocally since the CH_2 resonance signals of the COD ligand lay in the same region (δ 2.40–2.43). In the FTIR spectra obtained for the series, the presence of a band around 1620 cm^{-1} was ascribed to the remaining NH bond. However, no NH signal was observed from the ^{1}H NMR spectra, similar behaviour was described for a Rh(III) complex.[17] The molecular structure of complex **Ir1A** was determined by X-ray crystallography, corroborating the above assignments, in agreement with the monomeric nature of the complexes.

When the reactions were run in basic medium, typically an organic solvent with addition of NEt_3, monomeric complexes were also obtained; namely **M2A–C**. (Scheme 1, reaction ii). The same complexes were formed both when the complexes were obtained by reaction of the monomeric precursor **M1A–C** and by direct reaction of the dimeric precursor $[M(\mu\text{-Cl})(COD)]_2$. As expected, pyrimidinethiol and derivatives acted in their deprotonated form, as a thionate, (thus indicating their original thione-like structure), simultaneously bonded to the metal atom through the sulfur atom and one nitrogen atom. Although the crystals obtained were not amenable to X-ray study, the nature of the chelating complex was clarified by means of both FTIR and ^{1}H NMR studies. From the FTIR spectra obtained, no νNH or νSH vibration bands were observed. The bands present in the free ligands and in the complexes of series **M1A–C** centred around 1620 cm^{-1} disappeared. The bands in region I were displaced to lower frequencies while bands in region III and IV were blue-shifted. This is a general trend observed for all the complexes of the **M2A–C** series. These trends observed for the FTIR band displacements are in good agreement with the chelating nature of the thiopyrimidine ligand in these complexes.[18] The ^{1}H NMR spectra of the **Rh2A** and **Ir2A** complexes show that the methyl groups are non-equivalent at r.t. Two signals for the iridium complexes at δ 2.36 and 2.50, and one broad signal for the rhodium complex at δ *ca.* 2.41, which can be attributed to the formation of chelating type complexes, were observed. In the case of the rhodium complexes, a fluxional behaviour could be proposed since the methyl signals were present in the form of a broad six proton signal. For the non-methylated thionate complexes, the ^{1}H NMR spectra show three signals in the aromatic region at δ 8.71, 8.65 and 7.26 for the **Ir2C** complex, in accordance with a chelating type structure. The resonance centred at δ 7.26 was assigned to the central proton of the pyrimidine ring, the signals at lower field being assigned to the protons adjacent to the N atoms.[19] For complex **Rh2C** only two signals δ 8.49 and 7.05 were observed in the spectra. This is in

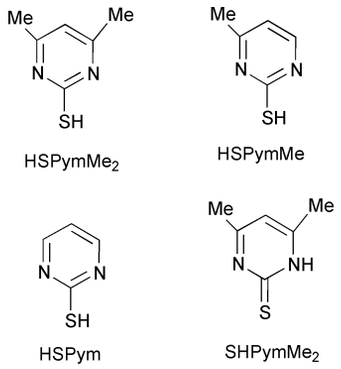

Fig. 2 Summary of the ligands described in this article.

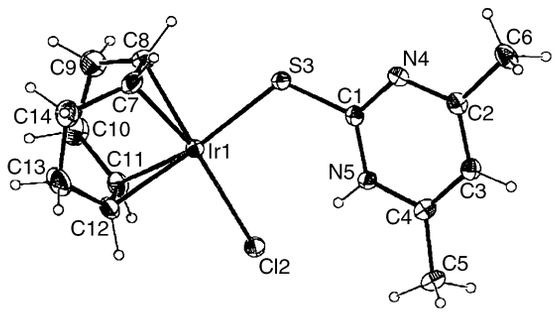

Fig. 3 An ORTEP representation of the structure of complex [Ir(HSPymMe$_2$)(Cl)(COD)] **Ir1A** showing the atom labelling scheme.

Table 1 Selected bond lengths (Å) and angles (°) for complex [Ir(HSPymMe$_2$)(Cl)(COD)] **Ir1A**

Ir(1)–C(11)	2.114(6)	S(3)–C(1)	1.719(6)
Ir(1)–C(8)	2.112(6)	N(4)–C(1)	1.333(7)
Ir(1)–C(12)	2.120(5)	N(4)–C(2)	1.352(7)
Ir(1)–C(7)	2.119(6)	N(5)–C(4)	1.349(7)
Ir(1)–S(3)	2.342(2)	N(5)–C(1)	1.352(7)
Ir(1)–Cl(2)	2.382(2)	C(2)–C(3)	1.377(8)
C(11)–Ir(1)–C(8)	81.2(3)	C(11)–Ir(1)–C(12)	38.7(3)
C(8)–Ir(1)–C(12)	95.2(3)	C(11)–Ir(1)–C(7)	93.0(3)
C(8)–Ir(1)–C(7)	40.0(3)	C(12)–Ir(1)–C(7)	81.0(2)
C(11)–Ir(1)–S(3)	157.3(2)	C(8)–Ir(1)–S(3)	84.5(2)
C(12)–Ir(1)–S(3)	161.5(2)	C(7)–Ir(1)–S(3)	87.0(2)
C(11)–Ir(1)–Cl(2)	88.4(2)	C(8)–Ir(1)–Cl(2)	159.8(2)
C(12)–Ir(1)–Cl(2)	87.2(2)	C(7)–Ir(1)–Cl(2)	159.1(2)
S(3)–Ir(1)–Cl(2)	99.54(6)	C(1)–S(3)–Ir(1)	119.2(2)
C(1)–N(4)–C(2)	117.5(4)	C(4)–N(5)–C(1)	123.4(5)
N(4)–C(1)–N(5)	120.7(5)	N(4)–C(1)–S(3)	117.0(4)
N(5)–C(1)–S(3)	122.3(4)	N(4)–C(2)–C(3)	122.3(5)
N(4)–C(2)–C(6)	115.2(5)	C(3)–C(2)–C(6)	122.5(5)
C(4)–C(3)–C(2)	119.5(5)	N(5)–C(4)–C(3)	116.4(5)
N(5)–C(4)–C(5)	117.9(5)	C(3)–C(4)–C(5)	125.7(5)

accordance with the fluxional behaviour of the thiopyrimidine ligand. The monomethylated complexes were not sufficiently soluble to perform an accurate NMR analysis.

The synthesis pathway is depicted in Scheme 1, and the structure and abbreviations are summarised in Fig. 2.

The crystal structure of [IrCl(HSPymMe$_2$)(COD)] Ir1A

The molecular structure of complex **Ir1A** was determined by X-ray diffraction. Selected bond distances and angles are given in Table 1 with the ORTEP[20] representation shown in Fig. 3. The compound crystallizes in the triclinic group $P\bar{1}$ with $Z = 2$. Atom Ir(I) is bonded to the thione ligand through the sulfur atom. The N–*H* lies close to the Cl atom, which is coordinated to the Ir atom. Despite their suitable special arrangement, no Cl···HN interactions are expected in the solid state, since the distance is 2.20(6) Å. The Ir–S distance is 2.342(2) Å, lower than that observed for the pyridine-thiolate complex

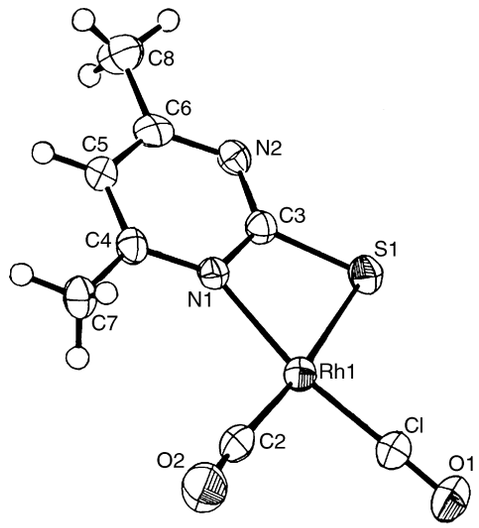

Fig. 4 An ORTEP representation of the structure of complex [Rh(SPymMe$_2$)(CO)$_2$] **Rh3A** showing the atom labelling scheme.

[IrH$_2$(SPy)$_2$(PPh$_3$)$_2$] [2.497(9) Å].[21] This is in accordance with a double bond character of the Ir–S bond for **Ir1A**, since the pyrimidine ligand is protonated. Furthermore, the N(4)–C(1) bond is shorter than the N(5)–C(1) bond and the values of angles C(1)–N(4)–C(2) and C(1)–N(5)–C(4) are 117.5(4) and 123.4(5)°, lower and higher than 120°, respectively, as expected for protonated and non-protonated N atoms, respectively.[22] The Ir(1)–S(3)–C(1) angle value of 119.2(2)°, close to 120°, is expected for a pure sp^2 hybridisation.

Synthesis of carbonyl complexes

When CO was bubbled through an acetone solution/suspension of the aforementioned complexes **M2A–C**, *cis*-dicarbonyl chelating complexes were obtained (Scheme 1, reaction iii). The structure of complex **Rh3A** was successfully resolved by X-ray diffraction. The complex displays a square planar structure with the CO ligands adopting a *cis* disposition around the Rh atom. The thiopyrimidine ligand is chelating the metal atom. FTIR spectra obtained from these complexes display a similar type of behaviour in the "-N=C=S" region to that of the parent ones. The bands in region I are displaced to lower wavenumbers, while bands in region III and IV are displaced to higher wavenumbers when compared with those of the free ligand. The ^{1}H NMR of the **M3A** complex reveals that both methyl groups are non-equivalent, in accordance with a chelating-like behaviour of the thiopyrimidine ligand. The complexes **Ir3B**, **Rh3C** and **Ir3C** were highly insoluble in the common deuterated solvents and hence an accurate study of them by NMR was not possible. Again, keeping in mind that **Rh3A** is a bis-carbonyl-chelating square planar monomer complex (determined by X-ray diffraction) the structure of the other carbonyl complexes of the series can be proposed to be similar to the structure of the complex **Rh3A**, since the FTIR and ^{1}H NMR data (where available) obtained are analogous to that obtained for **Rh3A**.

Crystal structure of [Rh(SPymMe$_2$)(CO)$_2$] Rh3A

The structure of **Rh3A** was determined by X-ray diffraction from a two-dimensional metal-like solid. The ORTEP[20] representation is shown in Fig. 4. Selected bond angles and distances are given in Table 2. A square planar structure around the Rh atom, with the thiopyrimidine ligand acting as a chelate was obtained. The CO ligands adopt a *cis*-disposition around the rhodium atom. The low S–Rh–N angle value, 69.4(1)°, is indicative of the strong contraction intrinsic to this type of complexes. Similar distances were found for both R–C bonds

Table 2 Selected bond lengths (Å) and angles (°) for complex $[Rh(SPymMe_2)(CO)_2]$ **Rh3A**

Rh(1)–S(1)	2.361(2)	Rh(1)–N(1)	2.078 (4)
Rh(1)–C(1)	1.845 (6)	Rh(1)–C(2)	1.875 (7)
S(1)–C(3)	1.750 (5)	O(1)–C(1)	1.131 (7)
O(2)–C(2)	1.135 (7)	N(1)–C(3)	1.345 (6)
N(1)–C(4)	1.360 (6)	N(2)–C(3)	1.326 (7)
N(2)–C(6)	1.356 (7)	C(4)–C(5)	1.373 (7)
C(4)–C(7)	1.480 (8)	C(5)–C(6)	1.379 (7)
S(1)–Rh(1)–N(1)	69.4(1)	S(1)–Rh(1)–C(1)	98.0(2)
S(1)–Rh(1)–C(2)	173.1(2)	N(1)–Rh(1)–C(1)	167.4(2)
N(1)–Rh(1)–C(2)	103.7(2)	C(1)–Rh(1)–C(2)	88.9(3)
Rh(1)–S(1)–C(3)	80.0(2)	Rh(1)–N(1)–C(3)	101.1(3)
Rh(1)–N(1)–C(4)	140.4(4)	C(3)–N(1)–C(4)	118.4(4)
C(3)–N(1)–C(6)	115.2(4)	Rh(1)–C(1)–O(1)	178.2(6)
Rh(1)–C(2)–O(2)	175.6(5)	S(1)–C(3)–N(1)	109.4(4)
S(1)–C(3)–N(2)	124.2 (4)	N(1)–C(3)–N(2)	126.4(4)
N(1)–C(4)–C(5)	118.2 (5)	N(1)–C(4)–C(7)	118.1(5)
C(5)–C(4)–C(7)	123.7 (8)	C(4)–C(5)–C(6)	120.0(5)
N(2)–C(6)–C(5)	121.9 (5)	N(2)–C(6)–C(8)	116.7(5)

[1.845(6) and 1.875(7) Å] from the CO ligands in a *trans*-position to the N and S atoms respectively. The monomer structure of the complexes of this series may be due to the influence of the nature of the ligand. When thiopyridine ligands were studied, dimeric complexes were obtained, as reported by Oro and co-workers for the complex $[\{Rh(\mu\text{-}Spy)(CO)_2\}]_2$.[23]

Synthesis of phosphinated derivatives

Monophosphinated complexes **M4A–C** were obtained from the reaction of the *cis*-dicarbonyl compounds **M3A–C** and PPh_3 in acetone at r.t. (Scheme 1, reaction iv). The results of the ^{1}H NMR spectra obtained for the dimethylated complexes are in accordance with the chelating behaviour of the thiopyrimidine ligands, since both methyl groups are non-equivalent. The FTIR spectra obtained for these complexes are also in agreement with a chelating ligand behaviour (red and blue shifts in regions I, III and IV, respectively, as compared with those obtained for the free ligand). Similar spectroscopic data to those obtained for **Rh4A** were recorded for the other members of the series. Thus a similar structure may be expected for all these complexes. The position of the FTIR bands in the CO region was carefully measured for the series of rhodium derivatives. As the number of methyl groups increases, the position of the CO band shifts to lower frequencies, consistent with greater donor ability from the ligand to the metal, which displaces more electronic density in the antibonding orbital of the CO molecule (π* backbonding), hence lowering the vibrational frequency of the CO molecule.[24] This feature was taken as indicative of the donor ability (basicity) of the pyrimidine ligand and will be of great interest in the catalytic testing of these molecules. This aspect will be further discussed in the section on catalytic activity.

Both **Rh4A** and **Ir4A** may accommodate a second PPh_3 molecule within their coordination sphere, affording **Rh5A** and **Ir5A** complexes, respectively, without displacement of the CO molecule. The CO bands seen in the FTIR spectrum were shifted to lower frequencies, from 1968 and 1954 cm^{-1} to 1942 and 1925 cm^{-1} respectively, consistent with the presence of a σ-donor ligand. The methyl group signals detected by ^{1}H NMR are centred at δ 2.22 and 2.06, respectively, for **Rh5A** and **Ir5A**. In both cases, only one signal was observed for the two methyl groups; this indicates a free rotation of the S–M bond at r.t.

The crystal structure of$[Rh(SPymMe_2)(CO)(PPh_3)]$ Rh4A

The crystal structure of the **Rh4A** complex was reported by one of us within his PhD Thesis in 1999[25] Very recently, Dahlenburg and Kühnlein[26] reported the synthesis and characterisation of the $[Rh(SPymMe_2)(CO)(PPh_3)]$ complex by a different reaction path to the one described here. Slight differences between the crystal structures of both complexes were observed. The CO ligands display a *trans*-disposition with respect to the S atom, while the PPh_3 adopts a *cis*-disposition with respect to the N atom.[27] The low S–Rh–N angle value, 68.8(7)°, is indicative of the strong contraction, which in turn is intrinsic to this type of complex.

Reaction with O_2

Mono- and di-phosphinated iridium derivatives, **Ir4A** and **Ir5A**, seem to be unstable in air, affording pale yellow complexes after just a few hours of exposure. When O_2 was bubbled through a solution of these complexes, the dioxygen complexes **Ir6A** and **Ir7A**, respectively, were obtained (Scheme 1, reaction v). A shift towards higher wavenumbers values was observed for the CO band in both complexes: from 1954 and 1925 cm^{-1} up to 1998 and 1934 cm^{-1}, respectively. In addition, a band centred at 842 cm^{-1}, attributable to peroxo species νO–O,[28] was detected. The methyl groups were non-equivalent in the ^{1}H NMR spectra. This may be considered as proof of the chelating nature of the pyrimidine ligand.

Catalytic activity

The hydroformylation of 1-heptene was accomplished with some of the Rh complexes described above. Our studies focused on: (i), the effect that the electronic density in the rhodium centre may have in their catalytic behaviour. Varying the number of methyl substituents on the pyrimidine-thiolate ligands, their donor capacity was modulated; (ii), the effect of the phosphine, both intrinsic – catalysts with and without triphenylphosphine were studied – and extrinsic; and (iii), the effect of the reaction conditions, such as total pressure, and solvent polarity. It is well known that the presence of triphenylphosphine in the reaction medium increases selectivity towards linear aldehydes, decreasing the reaction rate.[29] However, there are several exceptions to this trend.[30] There are not many hydroformylation rhodium catalysts that contain only sulfur derivatives as the hetero-donor ligands active in the hydroformylation reaction.[31]

The alkene used was 1-heptene and, unless indicated, the solvent was toluene. The reactions conditions used were: 30 bar $CO : H_2 = 1 : 1$ (molar), 343 K and 750 tpm (turns per minute). Samples were analysed at regular intervals by liquid-gas chromatography.

In order to examine ligand effect, the complexes **Rh4A**, **Rh4B** and **Rh4C** were studied for the hydroformylation reaction of 1-heptene under similar reaction conditions. As previously stated, the main difference between these complexes is the number of methyl groups in the pyrimidine ligand. By means of FTIR spectroscopy, the CO band position was correlated with the electronic density of the rhodium centre. As the number of methyl groups rose, the position of the CO band shifted to lower frequency values. This trend was consistent with a major increase in the donor ability of the pyrimidine ligands as the number of methyl groups increased. The conversion profiles are shown in Fig. 5 and follow typical S-shaped curves, achieving conversions as high as 99%. As seen in Fig. 5, variation in the activation period is the main difference between the three catalytic reactions. As the donor ability of the pyrimidine ligand rises, or in other words, as the number of methyl groups of the thiopyrimidine ligand increases, (**Rh4A** > **Rh4B** > **Rh4C**), the induction period decreases. This can be tentatively ascribed to an easier generation of some kind of rhodium hydride species as the rhodium electronic density was increased. During the hydroformylation of 1-heptene, with all three catalysts, aldehyde was the main product detected (up to 95%) the n : i ratio being close to 3.2 for all the catalyst precursors. When the **Rh4C** complex was the catalyst precursor, a certain degree of 1-heptene isomerisation was detected.

Table 3 Effect of the catalyst in the hydroformylation of 1-heptene

	Conversion[a]	Time/min	TOF[b]	% Aldehyde[c]	n/i[d]	PPh_3[e]
Rh4A	99.3	335	150	99.8	3.6	0
Rh4B	99.3	400	79	98.8	3.1	0
Rh4C	99.4	367	47	95.9	3.4	0
Rh4A	97.6	326	63	98.6	3.9	1
Rh4A	97.2	423	59	99.2	2.8	3
Rh4A	99.7	387	43	99.5	2.9	10
Rh4A	99.1	303	84	99.4	3.0	20
Rh4C	99.5	197	87	99.7	3.2	1
Rh4C	94.5	202	75	100	4.3	2
Rh4C	99.4	162	99	99.5	3.5	3

[a] 1-Heptene conversion (%) [b] Maximum turnover frequency achieved in the reaction, defined as number of mol of aldehyde formed per mol of catalyst per hour. [c] Aldehyde selectivity (total yield of aldehyde formed per mol of 1-heptene converted). [d] Mol ratio of *n*-octanal/internal aldehydes. [e] Equivalents added.

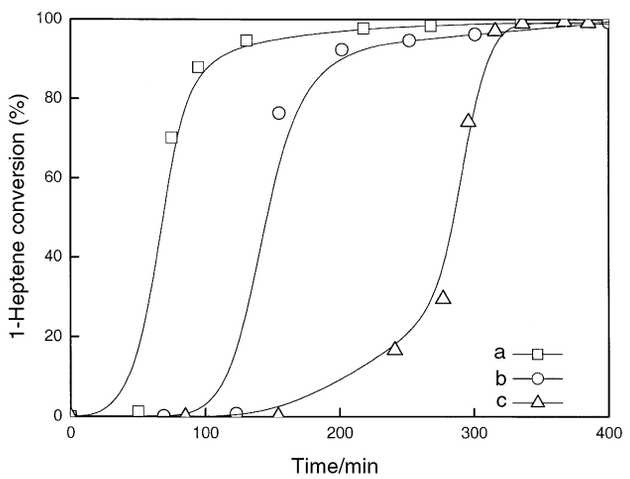

Fig. 5 Effect of the catalyst precursor in the 1-heptene hydroformylation reaction at 70 °C and 30 bar (H_2 : CO = 1 : 1): (a) complex **Rh4A** as catalyst, (b) complex **Rh4B** as catalyst and (c) complex **Rh4C** as catalyst.

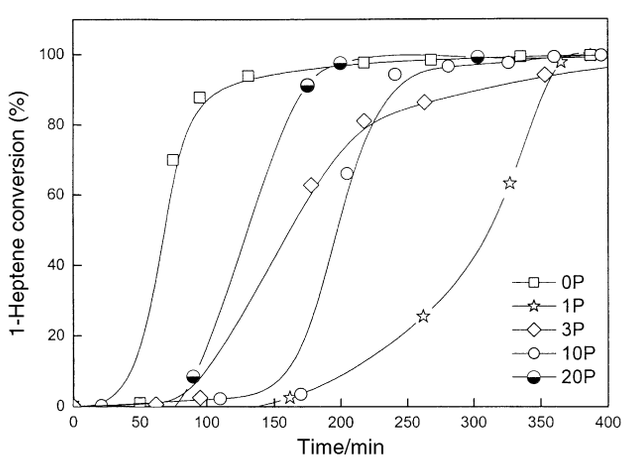

Fig. 6 Effect of the PPh_3 : Rh molar ratio on the hydroformylation reaction of 1-heptene conducted with catalyst **Rh4A**.

The addition of free phosphine (PPh_3/Rh = 1–20 : molar ratio) to the reaction medium modified the catalytic behaviour of the **Rh4A** complex, slowing the reaction rate. However, when a large amount of triphenylphosphine (20 mol PPh_3/mol Rh) was added to the reaction medium, the reaction was accelerated. Surprisingly, the presence of free triphenylphosphine in the reaction medium elicited a decrease in the n : i ratio, even though total aldehyde production was not found to be dependent on the amount of triphenylphosphine added. The activity profiles are shown in Fig. 6.

When the **Rh4C** complex was used as the catalyst precursor, the presence of free triphenylphosphine in the reaction medium increased both the reaction rate and selectivity towards n-octanal.

When the **Rh3A** complex was used as catalyst, the hydroformylation reaction did not take place. Instead, a certain degree of 1-heptene isomerization was observed. This supports the notion that PPh_3 is necessary for these complexes to accomplish the reaction. Indeed, when PPh_3 was added to **Rh3A**, hydroformylation of 1-heptene proceeded satisfactorily and the chemo- and regio-selectivities were similar to those obtained when **Rh4A** was used as catalyst.

Some selected kinetic data are offered in Table 3.

Effect of external reaction parameters

The effects of the total reaction pressure, temperature and the solvent used were assessed for the **Rh4A** complex as a catalyst. The effect of total pressure was evaluated by performing the reaction at 30 and 8 bar of H_2/CO (mol : mol = 1 : 1). When the reaction took place at 8 bar, it slowed down considerably and total conversion was only achieved after 23 h. At low pressure some gas diffusional phenomena may dominate the reaction pathway. Again, aldehyde production was dominant, with an n : i ratio of about 4 at maximum conversion, even though the total amount of aldehydes was *ca.* 85%, lower than in the case of the reaction performed at higher pressure. When the reaction was conducted in the presence of free triphenylphosphine (PPh_3 : Rh = 1 : 1 molar), total conversion was achieved faster than in the former reaction. Moreover, the total amount of aldehydes was higher and the chemoselectivity of the reaction was *ca.* 98%.

When the reaction was performed in acetone as solvent, no significant differences were found with respect to the product distribution achieved for the reaction conducted in toluene. However, the reaction became much slower, achieving total conversions only after long periods of time. When the reaction was carried out in the presence of external PPh_3 (PPh_3 : Rh = 1 : 1 molar), no significant changes were observed, the reaction rate being slightly lowered. However, when the reaction was conducted at lower pressure (8 bar H_2 : CO = 1 : 1 molar), the reaction rate decreased considerably and after 24 h a conversion of only *ca.* 50% was achieved, even though the n : i ratio was 10 : 1.

When the reaction was performed in polar proton-donor solvents such as methanol and ethanol, the reaction rates were similar to those seen when the reaction was accomplished in toluene; when the reaction was conducted in acetone, the rate was slightly lower than when it was conducted in toluene. However, the distribution of the reaction products was different. In the oxygenated solvents, long-chain condensation products, mainly acetals and hemiacetals, were detected. These products were formed more favourably when the reaction solvent was ethanol, yielding *ca.* 20% of the total product

Table 4 Hydroformylation of 1-heptene cayalysed by **Rh4A**

	Conversion[a]	Time/min	Q_{sel}[b]	Solvent	Pressure[c]	n/i[d]	PPh_3[e]
Rh4A	95	1420	84.8	Toluene	8	4.5	0
Rh4A	98	360	95.6	Toluene	8	4.2	1
Rh4A	91	370	100	Acetone	30	4.5	0
Rh4A	99	453	100	Acetone	30	4.1	1
Rh4A	53	1426	99	Acetone	8	10	1
Rh4A	99	305	90	MeOH	30	3.7	0
Rh4A	100	560	60	EtOH	30	52	0

[a] 1-Heptene conversion (%). [b] Chemoselectivity (% of aldehydes formed). [c] Total reduction pressure in bar. [d] Mol ratio of *n*-octanal/internal aldehydes. [e] Equivalents added.

obtained in the reaction. The appearance of long-chain oxygenated compounds during the hydroformylation of 1-hexene in ethanol by means of Rh-type catalysts has been reported previously by Alvila *et al.*,[32] although no proper identification of the products was offered. In both cases, the alkene isomerization by-products were as low as 2–3%.

Some selected kinetic data are depicted in Table 4.

Conclusions

The reaction of dimeric rhodium and iridium complexes with pyrimidinethiolate derivatives affords monomeric complexes. The coordination of the ligands to the metal atoms depends on the nature of the solvent used. In basic solvents, chelating-type complexes are formed. Dimethylated derivatives are generated more readily than mono- and non-methylated derivatives, and their higher solubility in organic solvents make them excellent candidates for their study in the liquid phase. The complexes may be carbonylated and phosphinated, thus yielding catalysts for the hydroformylation reaction. The effect of the donor capacity of the complexes is correlated with the reaction rate, although it does not correlate in a lineal fashion with the selectivity towards aldehydes, even though the lowest n : i ratio was obtained with the **Rh4C** catalyst, as expected from previous studies. The presence of PPh_3 is necessary in order to obtain aldehydes. However, no linear effect was found between the amount of PPh_3 and the activity or selectivity of the reaction. While for the most basic catalyst, **Rh4A**, the reaction rate appears to decrease with the amount of PPh_3, the opposite effect was observed for the **Rh4C** catalyst. In this latter case, this would be in good agreement with the necessity of a greater donor capacity of the ligands towards the metal centre for the hydroformylation reaction to be achieved.

Experimental

Materials and measurements

All reactions were carried out under nitrogen using Schlenk techniques. Solvents were dried and deoxygenated prior to use. Pyrimidine-2-thione, 2-mercapto-4-methylpyrimidine, 4,6-dimethyl-2-mercaptopyrimidine, designated throughout this paper as: HSPym, HSPymMe and $HSPymMe_2$, respectively, and NEt_3 were purchased from Aldrich and were used without further purification. PPh_3 was purchased from Aldrich and was crystallised in previously degassed EtOH. $[Rh(\mu\text{-}Cl)(COD)]_2$ and $[Ir(\mu\text{-}Cl)(COD)]_2$ were prepared from $RhCl_3 \cdot H_2O$ and $(NH_4)_2[IrCl_6]$, respectively, according to previously described methods.[33] CO (N 45) was used directly from a cylinder. FTIR spectra were recorded as KBr pellets on a Nicolet 5ZDX spectrometer. ^1H and ^{31}P NMR spectra were obtained on either 200 Gemini or 300 MHz Varian Fourier transform spectrometers. Trace amounts of protiated solvents were used as references and chemical shifts are reported in units of parts per million relative to $SiMe_4$.

Preparation of compounds

[Rh(HSPymMe$_2$)Cl(COD)] Rh1A. Acetone (20 ml) was added to a mixture of $HSPymMe_2$ (0.0569 g, 0.4056 mmol) and $[Rh(\mu\text{-}Cl)(COD)]_2$ (0.1 g, 0.2030 mmol). The solution was stirred at room temperature for 3 h. A yellow solid was filtered and crystallised from acetone–hexane. Yield 85%. FTIR (ν_{max}/cm^{-1}) (I) 1617s, 1565vs; (II) 1471w, 1370w; (III) 1232vs, 1212s, (IV) 979m. ^1H NMR (acetone-d_6): δ 1.82–1.87 (m, 8 H, COD); 2.04–2.06 (br, 6H, Me); 4.2 (m, 4H, COD); 6.97 (s, 1H, pym). $C_{14}H_{20}ClN_2RhS$ requires C, 43.5; H, 5.2; N, 7.2. Found: C, 43.0; H, 4.9; N, 7.2%.

[Rh(SPymMe$_2$)(COD)] Rh2A. NEt_3 (57 μl, 0.408 mmol) was added to an acetone solution of $[Rh(\mu\text{-}Cl)(COD)]_2$ (0.1 g, 0.203 mmol) and $HSPymMe_2$ (0.056 g, 0.408 mmol). After 3 h of stirring, a yellow solid was filtered and washed with water three times and crystallised from acetone–hexane. Yield 85%. FTIR (ν_{max}/cm^{-1}) (I) 1583f, 1528m; (II) 1430m, 1339m; (III) 1248vs; (IV) 875m. ^1H NMR (acetone-d_6): δ 1.85–1.99 (d, 8 H, COD); 2.08–2.17 (m, 6H, Me); 4.49 (m, 4H, COD); 6.59 (s, 1H, pym). $C_{14}H_{19}N_2RhS$ requires C, 48.0, H, 5.5; N, 8.0. Found: C, 48.0, H, 5.4; N, 7.9%.

[Rh(SPymMe$_2$)(CO)$_2$] Rh3A. CO was bubbled through a solution of **Rh2A** (0.05 g, 0.1424 mmol) in acetone (15 ml) for 20 min. The solution was stirred at room temperature. A brown-metallic solid appeared immediately. A crystalline metal-like solid was filtered off and washed with hexane. Yield 99%. FTIR (ν_{max}/cm^{-1}) (I) 1601m, 1526m; (II) 1438s; (III) 1266m (IV) 750w; (CO) 2085vs, 1992vs. ^1H NMR (acetone-d_6): δ 2.35, 2.36 (2s, 6H, Me); 6.90 (s, 1H, pym). $C_8H_7N_2O_2RhS$ requires C, 32.2; H, 2.3; N, 9.4. Found: C, 32.1; H, 2.0; N, 9.4%.

[Rh(SPymMe$_2$)(CO)(PPh$_3$)] Rh4A. Acetone (15 ml) was added to a mixture of **Rh3A** (0.1175 g, 0.394 mmol) and PPh_3 (0.5169 g, 0.394 mmol) and a vigorous production of CO was observed. The solution turned yellow while it was being stirred over 2 h. The solution was cooled and a yellow solid was filtered off. A crystalline solid was obtained from the mother-liquor. Yield 90%. FTIR (ν_{max}/cm^{-1}) (I) 1580m, 1534m; (II) 1437m; (III) 1269m; (IV) 753w; (CO) 1968vs. ^1H NMR (acetone-d_6): δ 2.27, 2.36 (2s, 6H, Me); 6.30 (s, 1H, pym); 7.5–7.7 (m, 15H, PPh_3). $C_{25}H_{22}N_2OPRhS$ requires C, 56.4; H, 4.2; N, 5.3. Found: C, 56.3; H, 4.1; N, 5.3%.

[Rh(SPymMe$_2$)(CO)(PPh$_3$)$_2$] Rh5A. Acetone (15 ml) was added to a mixture of **Rh4A** (0.0165 g, 0.031 mmol) and PPh_3 (0.0082 g, 0.031 mmol). The solution was stirred for 12 h. A yellow solid was filtered off and washed with diethyl ether. Yield 70%. FTIR (ν_{max}/cm^{-1}) (I) 1574m; (II) 1479m; (III) 1259s, 1091s; (CO) 1978m, 1942vs. ^1H NMR (acetone-d_6): δ 2.2 (s, 6H, Me); 6.65 (s, 1H, pym). $C_{44}H_{37}N_2OP_2RhS$ requires C, 64.3; H, 4.6; N, 3.4. Found: C, 64.5; H, 4.6; N, 3.5%.

[Ir(HSPymMe$_2$)Cl(COD)] Ir1A. This compound was prepared in a similar manner to **Rh1A** from [Ir(μ-Cl)(COD)]$_2$ (0.1 g, 0.148 mmol) and HSPymMe$_2$ (0.0422 g, 0.3 mmol). Suitable crystals for X-ray diffraction were obtained from the mother-liquor. Yield 75%. FTIR (ν_{max}/cm^{-1}) (I) 1619s, 1567vs; (II) 1469w, 1364w; (III) 1233vs, 1208s; (IV) 985m. ^{1}H NMR (acetone-d$_6$): δ 1.82–1.87 (m, 8 H, COD); 2.04–2.06 (m, 6H, Me); 4.2 (m, 4H, COD); 6.90 (s, 1H, pym). $C_{14}H_{20}ClIrN_2S$ requires C, 35.3; H, 4.2; N, 5.9. Found: C, 35.8; H, 3.9; N, 5.9%.

[Ir(SPymMe$_2$)(COD)] Ir2A. A red solid was obtained in a similar manner to **Rh2A** from **Ir1A** (0.27 g, 0.74 mmol) and NEt$_3$ (105 μl, 0.74 mmol). Yield 75%. FTIR (ν_{max}/cm^{-1}) (I) 1584s, 1526m; (II) 1429m; (III) 1249vs; (IV) 975w. ^{1}H NMR (acetone-d$_6$): δ 1.6, 1.8–2.2 (m, 8H, COD); 2.38 (s, 6H, Me); 3.78 (m, 4H, COD); 6.59 (s, 1H, pym). $C_{14}H_{19}IrN_2S$ requires C, 38.3; H, 4.4; N, 6.4. Found: C, 38.4; H, 4.3; N, 6.3%.

[Ir(SPymMe$_2$)(CO)$_2$] Ir3A. This solid was synthesised in a similar manner to **Rh3A** from **Ir2A** (0.05 g, 0.135 mmol) in acetone (15 ml). Yield 70%. FTIR (ν_{max}/cm^{-1}) (I) 1600m, 1526m; (II) 1439m; (III) 1269m; (IV) 746w; (CO) 2077vs, 1978vs. $C_8H_7IrN_2O_2S$ requires C, 24.8; H, 1.8; N, 7.3. Found: C, 24.8; H, 1.7; N, 7.24%.

[Ir(SPymMe$_2$)(CO)(PPh$_3$)] Ir4A. A yellow complex was obtained in a similar way to **Rh4A** from **Ir3A** (0.04 g, 0.103 mmol) and PPh$_3$ (0.027 g, 0.103 mmol) in acetone. Yield 90%. FTIR (ν_{max}/cm^{-1}) (I) 1581m, 1530m; (II)1435m; (III) 1272m; (IV) 749w; (CO) 1954vs. ^{1}H NMR (acetone-d$_6$): δ 2.24 (s, 6H, Me); 6.96 (s, 1H, pym); 7.46–7.70 (m, 15H, PPh$_3$). $C_{25}H_{22}IrN_2OPS$ requires C, 48.3; H, 3.6; N, 4.5. Found: C, 48.2; H, 3.6; N, 4.6%.

[Ir(SPymMe$_2$)(CO)(O$_2$)(PPh$_3$)] Ir6A. A mixture of O$_2$/N$_2$ was bubbled through an **Ir4A** acetone solution for 60 min. A yellow solid, paler than the precursor, was obtained. Yield 95%. FTIR (ν_{max}/cm^{-1}) (I) 1583s, 1536m; (II) 1435m; (III) 1272m (IV) 714m; (CO) 1998vs; (O$_2$) 842. $C_{25}H_{22}IrN_2O_3PS$ requires C, 45.9; H, 3.4; N, 4.3. Found: C, 45.9; H, 3.2; N, 4.4%.

[Ir(SPymMe$_2$)(CO)(PPh$_3$)$_2$] Ir5A. This solid was obtained in a similar manner to **Ir4A** from **Ir3A** (0.0315 g, 0.082 mmol) and PPh$_3$ (0.0426 g, 0.163 mmol) in acetone (15 ml). A yellow solid was obtained and washed with ether. Yield 70%. FTIR (ν_{max}/cm^{-1}) (I) 1580s; (II) 1435s; (III) 1272w, 1094s; (IV) 749s; (CO) 1925s. $C_{43}H_{37}IrN_2OP_2S$ requires C, 58.4; H, 4.2; N, 3.2. Found: C, 58.5; H, 4.6; N, 3.2%.

[Ir(SPymMe$_2$)(CO)(O$_2$)(PPh$_3$)$_2$] Ir7A. O$_2$ was bubbled through an acetone solution of **Ir5A**. A yellow solid, paler than the precursor, was filtered off. Yield 65%. FTIR (ν_{max}/cm^{-1}) (I) 1580s; (II) 1437vs; (III) 1263m, 1094s; (IV) 747s; (CO) 1934. (O$_2$) 820w. $C_{43}H_{37}IrN_2O_3PS$ requires C, 55.9; H, 4.0; N, 3.1. Found: C, 56.3; H, 4.0; N, 3.1%.

[Rh(SPymMe)(COD)] Rh2B. NEt$_3$ (120 ml, 0.820 mmol) was added to an acetone (15 ml) solution of [Rh(μ-Cl)(COD)]$_2$ (0.1 g, 0.203 mmol) and HSPymMe·HCl (0.0667 g, 0.406 mmol). An orange solid was filtered off and washed with water, dried, and crystallised from acetone–hexane. Yield 70%. FTIR (ν_{max}/cm^{-1}) (I) 1567s, 1537s; (II) 1409s, 1320s; (III) 1262w, 1190s; (IV) 874m. $C_{13}H_{17}N_2RhS$ requires C, 46.6; H, 5.1; N, 8.3. Found: C, 46.6; H, 5.3; N, 8.1%.

[Rh(SPymMe)(CO)$_2$] Rh3B. This metal-like solid was prepared in the same manner to solid **Rh3A** from **Rh2B** (0.04 g, 0.1188 mmol) in acetone. Yield 75%. FTIR (ν_{max}/cm^{-1}) (I) 1570m, 1541m; (II) 1435m, 1308s; (III) 1237w, 1179w; (IV) 819w; (CO) 2078vs, 2052m, 2015vs, 1933m. $C_7H_5N_2O_2RhS$ requires C, 29.6; H, 1.8; N, 9.9. Found: C, 30.2; H, 1.9; N, 9.5%.

[Rh(SPymMe)(CO)(PPh$_3$)] Rh4B. This solid was prepared from **Rh3B** (0.048 g, 0.18 mmol) and PPh$_3$ (0.047 g, 0.18 mmol) in the same way as **Rh4A**. Yield 70%. FTIR (ν_{max}/cm^{-1}) (I) 1574m; (II) 1434m; 1318m; (III) 1256w 1187m; (IV) 794w; (CO) 1977vs. $C_{24}H_{20}N_2OPRhS$ requires C, 54.6; H, 4.0; N, 5.4. Found: C, 53.6; H, 4.4; N, 5.2%.

[Ir(SPymMe)Cl(COD)]·HCl Ir1B. Acetone (15 ml) was added to a mixture of [Ir(μ-Cl)(COD)]$_2$ (0.06 g, 0.0893 mmol) and HSPym·HCl (0.0293 g, 0.179 mmol). After 2 h of stirring, a red solution began to appear, followed by the formation of a yellow crystalline solid, which was filtered off and crystallised from acetone–hexane. Yield 75%. FTIR (ν_{max}/cm^{-1}) (I) 1620vs, 1583vs; (II) 1368s; (III) 1234m, 1169m; (IV) 1000m. $C_{13}H_{19}Cl_2IrN_2S$ requires C, 31.3; H, 3.8; N, 5.7. Found: C, 30.1; H, 3.8; N, 6.2%.

[Ir(SPymMe)(COD)] Ir2B. This compound was prepared in a similar manner to **Rh2B** from NEt$_3$ (94 μl, 0.62 mmol), [Ir(μ-Cl)(COD)]$_2$ (0.1 g, 0.148 mmol) and HSPymMe·HCl (0.0426 g, 0.30 mmol). The solid was washed with water and crystallized from acetone–ethanol. Yield 72%. FTIR (ν_{max}/cm^{-1}) (I) 1568vs, 1534s; (II) 1410s, 1324vs; (III) 1281w, 1193m; (IV) 998 m. $C_{13}H_{17}N_2IrS$ requires C, 36.6; H, 4.0; N, 6.6. Found: C, 36.1; H, 3.9; N, 6.4%.

[Ir(SPymMe)(CO)$_2$]·2Me$_2$CO Ir3B. This solid was obtained from **Ir2B** (0.05 g, 0.1215 mmol) in a similar reaction to **Ir3A**. Yield 65%. FTIR (ν_{max}/cm^{-1}) (I) 1585s, 1535s; (II) 1413s, 1321s; (III) 1280w, 1198s; (IV) 890w; (CO) 2056vs, 2021vs. $C_{10}H_{11}N_2IrO_3S$ requires C, 31.9; H, 3.6; N, 6.6. Found: C, 31.1; H, 3.2; N, 6.8%.

[Ir(SPymMe)(CO)(PPh$_3$)] Ir4B. This compound was prepared in a similar manner to **Ir4A** from **Ir3A** (0.04 g, 0.103 mmol) and PPh$_3$ (0.027 g, 0.103 mmol). Yield: 89%. FTIR (ν_{max}/cm^{-1}) (I) 1576s; (II) 1435s; (III) 1190m; (IV) 803 w; (CO) 2002s. $C_{24}H_{20}IrN_2OPS$ requires C, 47.7; H, 3.3; N, 4.6. Found: C, 47.0; H, 3.3; N, 4.6%.

[Rh(SPym)Cl(COD)] Rh1C. This solid was obtained in a similar manner to **Rh1A** and **Rh1B** from [Rh(μ-Cl)(COD)]$_2$ (0.06 g, 0.121 mmol) and HSPym (0.0278 g, 0.248 mmol) in acetone. Yield 69%. FTIR (ν_{max}/cm^{-1}) (I) 1598vs, 1576vs, 1566vs; (II) 1419w, 1330s; (III) 1222w, 1174s; (IV) 771s. $C_{12}H_{15}N_2RhS$ requires C, 40.2; H, 4.5; N, 7.8. Found: C, 40.2; H, 4.4; N, 7.8%.

[Rh(SPym)(COD)] Rh2C. This solid was obtained in a similar manner to **Rh2A** from [Rh(μ-Cl)(COD)]$_2$ (0.1 g, 0.203 mmol), HSPym (0.0406 g, 0.406 mmol) and NEt$_3$ (57 μl, 0.407 mmol) in acetone. Yield 70%. FTIR (ν_{max}/cm^{-1}) (I) 1563m; 1541m; (II) 1410s, 1324vs; (III) 1251w, 1175m; (IV) 978m. $C_{12}H_{15}N_2RhS$ requires C, 44.7; H, 4.7; N, 8.6. Found: C, 44.7; H, 4.8; N, 8.3%.

[Rh(SPym)(CO)$_2$] Rh3C. This solid was prepared in a similar reaction to **Rh3A** and **Rh3B** from **Rh2C** (0.04 g, 0.124 mmol). Yield 65%. FTIR (ν_{max}/cm^{-1}) (I) 1588s, 1535s; (II) 1413s, 1321s; (III) 1261w, 1198m; (IV) 890w; (CO) 2056vs, 2021vs. $C_6H_2N_2O_2RhS$ requires C, 26.6; H, 1.1; N, 10.3. Found: C, 24.1; H, 1.4; N, 11.9%.

[Rh(SPym)(CO)(PPh$_3$)] Rh4C. This solid was prepared in a similar way to **Rh4A** and **Rh4B** from **Rh3C** (0.025 g, 0.093 mmol) and PPh$_3$ (0.024 g, 0.093 mmol). Yield 65%. FTIR (ν_{max}/cm^{-1}) (I) 1576s, 1538m; (II) 1435s; (III) 1248w, 1190m; (IV)

810w; (CO) 1983vs. $C_{23}H_{18}N_2OPRhS$ requires C, 54.8; H, 3.6; N, 5.5. Found: C, 54.1; H, 3.6; N, 5.2%.

[Ir(HSPym)Cl(COD)] Ir1C. This product was obtained in a similar manner to **Ir1A** from $[Ir(\mu\text{-}Cl)(COD)]_2$ (0.06 g, 0.0893 mmol) and HSPym (0.0204 g, 0.179 mmol). Yield 65%. FTIR (ν_{max}/cm^{-1}) (I) 1561s, 1546m; (II) 1432s, 1374vs; (III) 1224m, 1187m; (IV) 820w. $C_{12}H_{16}ClIrN_2S$ requires C, 32.2; H, 3.6; N, 6.2. Found: C, 32.6; H, 3.6; N, 6.1%.

[Ir(SPym)(COD)] Ir2C. This product was obtained in a similar manner to **Ir2A** from $[Ir(\mu\text{-}Cl)COD]_2$ (0.1 g, 0.15 mmol) and HSPym (0.0338 g, 0.30 mmol) and NEt_3 (45 μl, 0.31 mmol). Yield 69%. FTIR (ν_{max}/cm^{-1}) (I) 1557m, 1539m; (II) 1371vs; (III) 1251m, 1181m; (IV) 900w. $C_{12}H_{15}IrN_2S$ requires C, 35.0; H, 3.7; N, 6.8. Found: C, 35.3; H, 3.8; N, 6.6%.

[Ir(SPym)(CO)$_2$]·2Me$_2$CO Ir3C. This solid was obtained from **Ir2C** (0.05 g, 0.1215 mmol) in a similar manner to **Ir3A** and **Ir3B**. Yield 65%. FTIR (ν_{max}/cm^{-1}) (I) 1571s, 1539s; (II) 1378vs; (III) 1257m, 1184m; (IV) 800w; (CO) 2098sh, 2059vs, 2023vs, 2016(sh). $C_{12}H_{15}IrN_2O_4S$ requires C, 30.3; H, 3.2; N, 6.0. Found: C, 29.3; H, 2.8; N, 6.4%.

[Ir(SPym)(CO)$_2$(PPh$_3$)] Ir4C. This solid was obtained in a similar mode to **Ir4A** and **Ir4B** from **Ir3C** (0.04 g, 0.154 mmol) and PPh_3 (0.0404 g, 0.154 mmol). Yield 70%. FTIR (ν_{max}/cm^{-1}) (I) 1561m, 1538m; (II) 1435s, 1375vs; (III) 1243m, 1180m; (IV) 748m; (CO) 2007s, 1963s. $C_{24}H_{18}IrN_2O_2PS$ requires C, 46.6; H, 3.1; N, 4.7. Found: C, 47.8; H, 3.2; N, 4.3%.

Catalysis experiments

Hydroformylation reactions were carried out in a 100 cm^3 stainless steel autoclave (Magnedrive Autoclave Engineers) The autoclave was evacuated for 2 h before a solution containing the appropriate amount of catalyst to achieve a final Rh concentration of 2×10^{-3} M, and PPh_3 when necessary, was introduced by suction. Carbon monoxide was then introduced (4 bar) and the mixture was warmed to the final reaction temperature. CO and H_2 were added up to reaction pressure (H_2 : CO = 1 : 1) The pressure in the autoclave was monitored from a transducer. Samples were removed periodically, cooled to −30 °C and analysed by gas-liquid chromatography in a Hewlett Packard HP 6890 chromatograph equipped with FID detector and a 30 m × 0.032 mm HP-Innowax column.

X-Ray data collection

Complex Ir1A. Suitable crystals were selected and mounted on a fine glass fiber with epoxy cement. Accurate unit-cell parameters were derived from the least-squares fit of the angular setting of 25 high-order reflections. The data collection was performed on a Nonius-Mach3 diffractometer equipped with a graphite monochromated Mo-Kα radiation ($\lambda = 0.71070$ Å) using a ω–2θ scan technique to a θ maximum value of 28°. Parameters for the collection and refinement of diffraction data are contained in Table 5. Intensities were corrected for Lorentz and polarization effects and absorption correction was based on a ψ scan.[34]

The structure was solved using direct methods [35] and refined first isotropically by full-matrix least-squares using the SHELXL-93 [36] program and then anisotropically by blocked full-matrix least squares for all the non-hydrogen atoms. The hydrogen atoms were included in calculated positions, except H1 which was located in the difference-Fourier map, and were refined isotropically.

Complex Rh3A. A yellow needlelike crystal of **Rh3A** having approximate dimensions of 0.03 × 0.05 × 0.34 mm was mounted on a glass fiber using Paratone N hydrocarbon oil. All measurements were made on a Siemens SMART [37] diffractometer with graphite monochromated Mo-Kα radiation. Cell constants and an orientation matrix, obtained from a least-squares refinement using the measured positions of 2359 reflections with $I > 10\sigma(I)$ in the range $3.00 < 2\theta < 45.00°$ correspond to a primitive monoclinic cell. The data were collected at a temperature of −95 ± 1 °C. The data were corrected for Lorentz and polarization effects. The structure was solved by direct methods and expanded using Fourier techniques.[38] The non-hydrogen atoms were refined anisotropically. Hydrogen atoms were included in idealized positions but not refined. Parameters for the collection and refinement of diffraction data are given in Table 6.

CCDC reference numbers 160865 and 160866.

See http://www.rsc.org/suppdata/dt/b1/b101915p/ for crystallographic data in CIF or other electronic format.

Table 5 Crystal data and structure refinement for **Ir1A**

Empirical formula	$C_{14}H_{20}ClIrN_2S$
Formula weight	476.03
Temperature/K	293(2)
Wavelength/Å	0.71070
Crystal system	Triclinic
Space group	$P\bar{1}$
a/Å	7.539(8)
b/Å	8.272(4)
c/Å	12.473(2)
α/°	81.78(3)
β/°	82.77(5)
γ/°	88.05(8)
V/Å^3	763.6(9)
Z	2
D_c/g cm^{-3}	2.070
μ(Mo-Kα)/cm^{-1}	90.42
Transmission range	0.614–1.000
F(000)	456
Crystal size/mm	0.5 × 0.3 × 0.2
Index ranges	$0 \le h\ 9, -10 \le k\ 10, -16 \le l \le 16$
Data/restraints/parameters	3675/0/176
Goodness-of-fit on F^2	0.718
Final R indices [$I > 2\sigma(I)$]	$R1 = 0.0253$, $wR2 = 0.0740$
R indices (all data)	$R1 = 0.0308$, $wR2 = 0.0857$
Largest diff. peak, hole/e Å^{-3}	0.604, −1.261

Table 6 Crystal data and structure refinement for **Rh3A**

Empirical formula	$RhSO_2N_2C_8H_7$
Formula weight	298.12
Crystal color, habit	Yellow, needlelike
Crystal dimensions/mm	0.03 × 0.05 × 0.34
Crystal system	Monoclinic
Space group	$P2_1/a$ (no. 14)
a/Å	6.9019(2)
b/Å	13.3935(4)
c/Å	11.25340(10)
β/°	103.257(2)
V/Å^3	1012.55(4)
Z	4
μ(Mo-Kα)/cm^{-1}	18.62
$F_{(000)}$	584.00
Cell determination (2θ range/°)	2359 (3.0–45.00)
No. of reflections measured	4869
No. observations [$I > 3.00\sigma(I)$]	1042
Goodness of fit indicator	0.96
$R = \Sigma F_o\| - \|F_c/\Sigma\|F_o\|$	0.027
$R_w = [(\Sigma(\|F_o\| - \|F_c\|)^2/\Sigma F_o^2)]^{1/2}$	0.028

Acknowledgements

We thank Prof. R. A. Andersen, University of California, Berkeley for his help and F. J. Hollander, of CHEXRAY, University of California, Berkeley for the crystal structure of **Rh3A**. We also acknowledge financial support from CICYT under Project QUI98-0877.

References

1 P. Kopfmaier, *Eur. J. Clin. Pharm.*, 1994, **47**, 1; R. V. Parish and S. M. Cottrill, *Gold Bull.*, 1987, **20**, 3; M. O. Senge, *Angew. Chem., Int. Ed. Engl.*, 1996, **35**, 1923.
2 G. Aullón and S. Álvarez, *Chem. Eur. J.*, 1997, **3**, 655.
3 E. S. Raper, *Coord. Chem. Rev.*, 1996, **153**, 199.
4 K. Brandt and W. S. Sheldrick, *Inorg. Chim. Acta*, 1998, **267**, 39; J. Romero, M. L. Durán, A. Rodriguez, J. A. García-Vázquez, A. Sousa, D. J. Rose and J. Zubieta, *Inorg. Chim. Acta*, 1998, **274**, 131; K. Brandt and W. S. Sheldrick, *J. Chem. Soc., Dalton Trans.*, 1996, 1237; R. Fandos, A. Lanfranchi, A. Otero, M. A. Pellinghelli, M. J. Ruiz and P. Terreros, *Organometallics*, 1996, 4725.
5 E. S. Raper, *Coord. Chem. Rev.*, 1996, **165**, 475.
6 A. Bader and E. Lindner, *Coord. Chem. Rev.*, 1991, **91**, 27; S. G. Murray and F. R. Hartley, *Chem. Rev.*, 1981, **81**, 365.
7 E. Spinner, *J. Chem. Soc.*, 1960, 1237; R. A. Jones and A. R. Katritzky, *J. Chem. Soc.*, 1958, 3610; S. Stoyanov, I. Petkov, L. Antonov, T. Stoyanova, P. Karagiannidis and P. Aslanidis, *Can. J. Chem.*, 1990, **68**, 1482.
8 D. D. Perrin, *Dissociation Constants of Organic Bases in Aqueous Solution*, Butterworths, London, 1965, p. 164.
9 S. R. Fletcher and A. C. Skapski, *J. Chem. Soc., Dalton Trans.*, 1973, 929; S. G. Rosenfield, S. A. Swedberg, S. K. Arora and P. K. Mascharak, *Inorg. Chem.*, 1986, **25**, 2109.
10 A. J. Deeming and M. N. Meah, *Inorg. Chim. Acta*, 1986, **117**, L13; A. J. Deeming, K. I. Hardcastle, M. N. Meah, P. A. Bates, H. M. Dawes and M. B. Hursthouse, *J. Chem. Soc., Dalton Trans.*, 1988, 227.
11 *Rhodium-Catalyzed Hydroformylation*, ed. P. W. N. M. van Leeuwen and C. Claver, Kluwer Academic Publishers, Dordrecht, 2000; Recent Achievements in Carbonylation Reactions; P. Kalck (guest editor), *J. Mol. Catal. A: Chem.*, 1999, **143**; *Applied Homogeneous Catalysis with Organometallic Compounds: A Comprehensive Handbook in two Volumes*, ed. B. Cornils and A. Herrmann, VCH Publishers, New York, 1996; F. Ungváry, *Coord. Chem. Rev.*, 1999, **188**, 236; F. Ungváry, *Coord. Chem. Rev.*, 1997, **167**, 233; F. Ungváry, *Coord. Chem. Rev.*, 1997, **167**, 129; M. Beller, B. Cornils, C. D. Frohning and C. W. Kohlpaintner, *J. Mol. Catal. A: Chem.*, 1995, **104**, 17.
12 J. C. Bayón, C. Claver and A. M. Masdeu-Bultó, *Coord. Chem. Rev.*, 1999, **193–195**, 73, and references therein.
13 C. P. Casey, G. T. Whiteker, M. G. Melville, L. M. Petrovich, J. A. Gavney Jr. and D. R. Powell, *J. Am. Chem. Soc.*, 1992, **114**, 5535; M. Kranenburg, Y. E. M. van der Burgt, P. C. J. Kamer, P. W. N. M. van Leeuwen, K. Goubitz and J. Fraanje., *Organometallics*, 1995, **14**, 3081; C. P. Casey and M. L. Petrovich, *J. Am. Chem. Soc.*, 1995, **117**, 6007; P. C. J. Kamer, J. N. H. Reek and P. W. N. M. van Leeuwen, *CHEMTECH*, 1998 , 27; L. A. van der Veen, M. D. K. Boele, F. R. Bergman, P. C. J. Kamer, P. N. M. van Leeuwen, K. Goubitz, H. Schenk and C. Bo, *J. Am. Chem. Soc.*, 1998, **120**, 11616.
14 W. R. Moser, C. J. Papile, D. A. Brannon, R. A. Duwell and S. J. Weininger, *J. Mol. Catal.*, 1987, **41**, 271; J. D. Unruh and J. R. Christenson, *J. Mol. Catal.*, 1982, **14**, 19.
15 C. N. R. Rao and R. Venkataraghavan, *Spectrochemica Acta*, 1962, **18**, 541; C. N. R. Rao, R. Ventkataraghavan and T. R. Kasturi, *Can. J. Chem.*, 1964, **42**, 36; E. S. Raper and J. L. Brooks, *J. Inorg. Nucl. Chem.*, 1977, **39**, 2163.
16 S. C. Jain and R. Rivest, *J. Inorg. Nucl. Chem.*, 1967, **29**, 2787.
17 A. J. Deeming and M. N. Meah, *Inorg. Chim. Acta*, 1986, **117**, L13.
18 G. Battistuzzi, A. B. Corradi, D. Dallari, M. Saladini and R. Battistuzzi, *Polyhedron*, 1998, **18**, 57; B. Singh, M. M. P. Rukhaiyar and R. J. Sinha, *J. Inorg. Nucl. Chem.*, 1997, **39**, 29.
19 K. Brandt and W. S. Sheldrick, *J. Chem. Soc., Dalton Trans.*, 1996, 1237.
20 C. K. Johnson, ORTEP, Report ORNL-5138, Oak Ridge National Laboratory, Oak Ridge, TN, 1996.
21 P. Mura and S. D. Robinson, *Acta Crystallogr., Sect. C*, 1984, **40**, 1798.
22 U. Ohms, H. Guth, A. Kutoglu and A. Scheringer, *Acta Crystallogr., Sect. B*, 1982, **38**, 831; A. Kvick and S. S. Booles, *Acta Crystallogr., Sect. B*, 1972, **28**, 3405.
23 M. A. Ciriano, F. Viguri, J. J. Pérez-Torrente, F. J. Lahoz, A. A. Oro, A. Tiripicchio and M. Tiripicchio-Camellini, *J. Chem. Soc., Dalton Trans.*, 1989, 25.
24 G. H. Olivé and S. Olivé, ed., in *The Chemistry of the Catalyzed Hydrogenations of Carbon Monoxide*, Springer-Verlag, New York, ch. 3, 1984.
25 S. Rojas. PhD Thesis, U. A. M. Madrid, Spain, December 1999.
26 L. Dahlenburg and M. Kühnlein, *Eur. J. Inorg. Chem.*, 2000, 2117.
27 J. H. Yamamoto, W. Yoshida and C. M. Jensen, *Inorg. Chem.*, 1991, **30**, 1353.
28 E. Mieczynska, A. M. Trzeciak, J. J. Ziolkowski and T. Lis, *J. Chem. Soc., Dalton Trans.*, 1995, 105; A. Antiñolo, I. Fonseca, A. Ortiz, M. J. Rosales, J. Sanz-Aparicio, P. Terreros and H. Torrens, *Polyhedron*, 1999, **18**, 959.
29 B. Cornils, *New Synthesis with Carbon Monoxide*, ed. J. Falbe, Springer Verlag, Weinheim, 1980, ch. 1.
30 R. M. Deshpande, B. M. Bhanage, S. S. Divekar and R. V. Chaudhari, *J. Mol. Catal.*, 1993, **78**, L37; R. M. Deshpande, S. S. Divekar, R. V. Gholap and R. V. Chaudhari, *J. Mol. Catal.*, 1991, **67**, 333.
31 C. Claver, S. Castillón, N. Ruiz, G. Delogu, D. Fabbri and S. Gladiali, *J. Chem. Soc., Chem. Commun.*, 1993, 1833; J. L. G. Fierro, M. Martínez-Ripoll, M. D. Merchán, A. Rodrígez, P. Terreros, H. Torrens and M. A. Vivar-Cerrato, *J. Organomet. Chem.*, 1997, **544**, 243.
32 L. Alvila, T. A. Pakkanen, T. T. Pakkanen and O. Krause, *J. Mol. Catal.*, 1992, **73**, 325.
33 G. Giordano and R. H. Crabtree, *Inorg. Synth.*, 1990, **28**, 89; R. H. Crabtree, *Synth. React. Inorg. Metal Org. Chem.*, 1982, **12**, 407.
34 A. C. T. North, D. C. Phillips and F. S. Mathews, *Acta Crystallogr., Sect. A*, 1968, **24**, 351.
35 A. Altomare, G. Cascarano, C. Giacovazzo, A. Guagliardi, M. C. Burla, G. Polidori and M. Camalli, *J. Appl. Crystallogr.*, 1994, 435.
36 G. M. Sheldrick, Program for the Refinement of Crystal Structures from Diffraction data, University of Göttingen, Göttingen, Germany, 1993.
37 SMART Area-Detector Software Package; Siemens Industrial Automation, Inc., Madison, WI, 1995.
38 DIRDIF92: P. T. Beurskens, G. Admiraal, G. Beurskens, W. P. Bosman, S. García-Granda, R. O. Gould, J. M. M. Smits and C. Smykalla, The DIRDIF program system, Technical Report of the Crystallography Laboratory, University of Nijmegen, The Netherlands, 1992.